Biomedical Optics EXPRESS

Optical configuration of pigmented lesion detection by frequency analysis of skin speckle patterns

Yael Bishitz,[1,3] Nisan Ozana,[1,3] Ariel Schwarz,[1] Yevgeny Beiderman,[1] Javier Garcia,[2] and Zeev Zalevsky[1,*]

[1]*Faculty of Engineering and the Nano Technology Center, Bar-Ilan University, Ramat-Gan 52900, Israel*
[2]*Departamento de O´ptica, Universitat de46100 Burjassot, Spain*
[3]*These authors contributed equally to the paper*
[*]*Zeev.Zalevsky@biu.ac.il*

Abstract: In this paper we present a novel approach of realizing a safe, simple, and inexpensive sensor applicable to pigmented lesions detection. The approach is based on temporal tracking of back-reflected secondary speckle patterns generated while illuminating the affected area with a laser and applying periodic pressure to the surface via a controlled vibration source. When applied to pigmented lesions, the technique is superior to visual examination in avoiding many false positives and resultant unnecessary biopsies. Applying a series of different vibration frequencies at the examined tissue and analyzing the 2-D time varying speckle patterns in response to the applied periodic pressure creates a unique signature for each and different pigmented lesion. Analyzing these signatures is the first step toward detection of malignant melanoma. In this paper we present preliminary experiments that show the validity of the developed sensor for the classification of pigmented lesions.

OCIS codes: (030.6140) Speckle; (280.0280) Remote sensing and sensors; (170.0170) Medical optics and biotechnology.

References and links

1. J. Y. Lin and D. E. Fisher, "Melanocyte biology and skin pigmentation," Nature **445**(7130), 843–850 (2007).
2. M. Watson, "Drugs in Clinical Development for Melanoma," Pharmaceut. Med. **26**(3), 171–183 (2012).
3. F. O. Nestle, S. Alijagic, M. Gilliet, Y. Sun, S. Grabbe, R. Dummer, G. Burg, and D. Schadendorf, "Vaccination of melanoma patients with peptide- or tumor lysate-pulsed dendritic cells," Nat. Med. **4**(3), 328–332 (1998).
4. A. H. Sam and J. T. H. Teo, *Rapid Medicine* (London: Wiley-Blackwell 2010)
5. A. L. Breton, M. Amini-Adle, G. Duru, N. Poulalhon, S. Dalle, and L. Thomas, "Overview of the use of dermoscopy in academic and non-academic hospital centres in France: a nationwide survey," J. Eur. Acad. Dermatol. Venereol. **28**(9), 1207–1213 (2014).
6. A. Garcia-Uribe, J. Zou, M. Duvic, J. H. Cho-Vega, V. G. Prieto, and L. V. Wang, "In vivo diagnosis of melanoma and nonmelanoma skin cancer using oblique incidence diffuse reflectance spectrometry," Cancer Res. **72**(11), 2738–2745 (2012).
7. C. Benvenuto-Andrade, S. W. Dusza, A. L. C. Agero, A. Scope, M. Rajadhyaksha, A. C. Halpern, and A. A. Marghoob, "Differences between polarized light dermoscopy and immersion contact dermoscopy for the evaluation of skin lesions," Arch. Dermatol. **143**(3), 329–338 (2007).
8. Y. Pan, D. S. Gareau, A. Scope, M. Rajadhyaksha, N. A. Mullani, and A. A. Marghoob, "Polarized and nonpolarized dermoscopy: the explanation for the observed differences," Arch. Dermatol. **144**(6), 828–829 (2008).
9. A. A. Marghoob, L. Cowell, A. W. Kopf, and A. Scope, "Observation of chrysalis structures with polarized dermoscopy," Arch. Dermatol. **145**(5), 618 (2009).
10. R. Satta, L. Fresi, and F. Cottoni, "Dermoscopic rainbow pattern in Kaposi's sarcoma lesions: our experience," Arch. Dermatol. **148**(10), 1207–1208 (2012).
11. S. Q. Wang, S. W. Dusza, A. Scope, R. P. Braun, A. W. Kopf, and A. A. Marghoob, "Differences in dermoscopic images from nonpolarized dermoscope and polarized dermoscope influence the diagnostic accuracy and confidence level: a pilot study," Dermatol. Surg. **34**(10), 1389–1395 (2008).
12. American Cancer Society (ACS), http://www.cancer.org/cancer/skincancer/melanoma

#253568 Received 9 Nov 2015; revised 14 Jan 2016; accepted 4 Feb 2016; published 24 Feb 2016

13. Z. Apalla, A. Lallas, G. Argenziano, C. Ricci, S. Piana, E. Moscarella, C. Longo, and I. Zalaudek, "The light and the dark of dermatoscopy in the early diagnosis of melanoma: facts and controversies," Clin. Dermatol. **31**(6), 671–676 (2013).
14. L. Zimmer, L. E. Haydu, A. M. Menzies, R. A. Scolyer, R. F. Kefford, J. F. Thompson, D. Schadendorf, and G. V. Long, "Reply to M. Perier-Muzet et al," J. Clin. Oncol. **32**(28), 3203–3204 (2014).
15. L. Lovatto, C. Carrera, G. Salerni, L. Alós, J. Malvehy, and S. Puig, "In vivo reflectance confocal microscopy of equivocal melanocytic lesions detected by digital dermoscopy follow-up," J. Eur. Acad. Dermatol. Venereol. **29**(10), 1918–1925 (2015).
16. J. Zhao, H. Zeng, D. McLean, S. Kalia, and H. Lui, "Recent Advances in Real-Time Raman Spectroscopy for In Vivo Skin Cancer Diagnosis," Optics in the Life Sciences, BT4A.6 (2015).
17. M. Amouroux, W. C. P. M. Blondel, F. Granel-Brocard, F. Marchal, and F. Guillemin, "A preliminary study on skin phantoms to test spatially resolved-diffuse reflectance spectroscopy as a tool to help diagnose cutaneous melanoma: A non-invasive measurement of Breslow index," Biomed. Mater. Eng. **18**(4-5), 339–343 (2008).
18. X. Jia, H. Huang, and R. Wang, "A novel edge detection in medical images by fusing of multi-model from different spatial structure clues," Biomed. Mater. Eng. **24**(1), 1289–1298 (2014).
19. C. A. Agudelo and T. Yamaoka, "Magnetic resonance imaging detection of an uncommon granuloma formation after endothelial progenitor cells transplantation," Biomed. Mater. Eng. **23**(6), 555–566 (2013).
20. G. Salerni, C. Carrera, L. Lovatto, J. A. Puig-Butille, C. Badenas, E. Plana, S. Puig, and J. Malvehy, "Benefits of total body photography and digital dermatoscopy ("two-step method of digital follow-up") in the early diagnosis of melanoma in patients at high risk for melanoma," J. Am. Acad. Dermatol. **67**(1), e17–e27 (2012).
21. J. A. Wolf, J. F. Moreau, O. Akilov, T. Patton, J. C. English 3rd, J. Ho, and L. K. Ferris, "Diagnostic inaccuracy of smartphone applications for melanoma detection," JAMA Dermatol. **149**(4), 422–426 (2013).
22. T. D. Wang and J. Van Dam, "Optical biopsy: a new frontier in endoscopic detection and diagnosis," Clin. Gastroenterol. Hepatol. **2**(9), 744–753 (2004).
23. J.-T. Oh, M.-L. Li, H. F. Zhang, K. Maslov, G. Stoica, and L. V. Wang, "Three-dimensional imaging of skin melanoma in vivo by dual-wavelength photoacoustic microscopy," J. Biomed. Opt. **11**(3), 034032 (2006).
24. H. Makhlouf, A. R. Rouse, and A. F. Gmitro, "Dual modality fluorescence confocal and spectral-domain optical coherence tomography microendoscope," Biomed. Opt. Express **2**(3), 634–644 (2011).
25. D. Huang, E. A. Swanson, C. P. Lin, J. S. Schuman, W. G. Stinson, W. Chang, M. R. Hee, T. Flotte, K. Gregory, and C. A. Puliafito, "Optical coherence tomography," Science **254**(5035), 1178–1181 (1991).
26. J. G. Fujimoto, C. Pitris, S. A. Boppart, and M. E. Brezinski, "Optical coherence tomography: an emerging technology for biomedical imaging and optical biopsy," Neoplasia **2**(1-2), 9–25 (2000).
27. A. L. Clark, A. M. Gillenwater, T. G. Collier, R. Alizadeh-Naderi, A. K. El-Naggar, and R. R. Richards-Kortum, "Confocal microscopy for real-time detection of oral cavity neoplasia," Clin. Cancer Res. **9**(13), 4714–4721 (2003).
28. P. E. Paull, B. J. Hyatt, W. Wassef, and A. H. Fischer, "Confocal laser endomicroscopy: a primer for pathologists," Arch. Pathol. Lab. Med. **135**(10), 1343–1348 (2011).
29. D. Zink, A. H. Fischer, and J. A. Nickerson, "Nuclear structure in cancer cells," Nat. Rev. Cancer **4**(9), 677–687 (2004).
30. S. A. Lelièvre, V. M. Weaver, J. A. Nickerson, C. A. Larabell, A. Bhaumik, O. W. Petersen, and M. J. Bissell, "Tissue phenotype depends on reciprocal interactions between the extracellular matrix and the structural organization of the nucleus," Proc. Natl. Acad. Sci. U.S.A. **95**(25), 14711–14716 (1998).
31. P. Jorgensen, N. P. Edgington, B. L. Schneider, I. Rupes, M. Tyers, and B. Futcher, "The size of the nucleus increases as yeast cells grow," Mol. Biol. Cell **18**(9), 3523–3532 (2007).
32. A. Garcia-Uribe, E. B. Smith, J. Zou, M. Duvic, V. Prieto, and L. V. Wang, "In-vivo characterization of optical properties of pigmented skin lesions including melanoma using oblique incidence diffuse reflectance spectrometry," J. Biomed. Opt. **16**(2), 020501 (2011).
33. M. Pirtini Çetingül and C. Herman, "Quantification of the thermal signature of a melanoma lesion," Int. J. Therm. Sci. **50**(4), 421–431 (2011).
34. A. Safrani, O. Aharon, S. Mor, O. Arnon, L. Rosenberg, and I. Abdulhalim, "Skin biomedical optical imaging system using dual-wavelength polarimetric control with liquid crystals," J. Biomed. Opt. **15**(2), 026024 (2010).
35. O. Aharon, I. Abdulhalim, O. Arnon, L. Rosenberg, V. Dyomin, and E. Silberstein, "Differential optical spectropolarimetric imaging system assisted by liquid crystal devices for skin imaging," J. Biomed. Opt. **16**(8), 086008 (2011).
36. L. Graham, Y. Yitzhaky, and I. Abdulhalim, "Classification of skin moles from optical spectropolarimetric images: a pilot study," J. Biomed. Opt. **18**(11), 111403 (2013).
37. Y. Bishitz, N. Ozana, Y. Beiderman, F. Tenner, M. Schmidt, V. Mico, J. Garcia, and Z. Zalevsky, "Noncontact optical sensor for bone fracture diagnostics," Biomed. Opt. Express **6**(3), 651–657 (2015).
38. Y. Beiderman, M. Teicher, J. Garcia, V. Mico, and Z. Zalevsky, "Optical technique for classification, recognition and identification of obscured objects," Opt. Commun. **283**(21), 4274–4282 (2010).
39. Z. Zalevsky, Y. Beiderman, I. Margalit, S. Gingold, M. Teicher, V. Mico, and J. Garcia, "Simultaneous remote extraction of multiple speech sources and heart beats from secondary speckles pattern," Opt. Express **17**(24), 21566–21580 (2009).

#253568 Received 9 Nov 2015; revised 14 Jan 2016; accepted 4 Feb 2016; published 24 Feb 2016

40. Y. Beiderman, R. Blumenberg, N. Rabani, M. Teicher, J. Garcia, V. Mico, and Z. Zalevsky, "Demonstration of remote optical measurement configuration that correlates to glucose concentration in blood," Biomed. Opt. Express **2**(4), 858–870 (2011).
41. N. Ozana, N. Arbel, Y. Beiderman, V. Mico, M. Sanz, J. Garcia, A. Anand, B. Javidi, Y. Epstein, and Z. Zalevsky, "Improved noncontact optical sensor for detection of glucose concentration and indication of dehydration level," Biomed. Opt. Express **5**(6), 1926–1940 (2014).
42. A. Shenhav, Z. Brodie, Y. Beiderman, J. Garcia, V. Mico, and Z. Zalevsky, "Optical sensor for remote estimation of alcohol concentration in blood stream," Opt. Commun. **289**, 149–157 (2013).
43. Y. Beiderman, I. Horovitz, N. Burshtein, M. Teicher, J. Garcia, V. Mico, and Z. Zalevsky, "Remote estimation of blood pulse pressure via temporal tracking of reflected secondary speckles pattern," J. Biomed. Opt. **15**(6), 061707 (2010).
44. Z. Zalevsky, I. Margalit, Y. Beiderman, A. Skaat, M. Belkin, R.-P. Tornow, V. Mico, and J. Garcia, "Remote and Continuous Monitoring of Intraocular Pressure Using Novel Photonic Principle," Invest. Ophthalmol. Vis. Sci. **53**(14), 1972 (2012).
45. I. Margalit, Y. Beiderman, A. Skaat, E. Rosenfeld, M. Belkin, R.-P. Tornow, V. Mico, J. Garcia, and Z. Zalevsky, "New method for remote and repeatable monitoring of intraocular pressure variations," J. Biomed. Opt. **19**(2), 027002 (2014).

1. Introduction

Pigmented lesions ("birthmarks," "nevus" or "nevi") are benign growths which are composed of melanocytes (i.e. containing skin cells) [1,2]. Melanocytes produce melanin, the dark pigment in skin. The greater concentration of melanocytes in nevi is responsible for the color of the lesion which contrasts with the remainder of the skin [2]. There are three main skin cancers types. These types include Basal cell carcinoma (BCC), squamous cell carcinoma (SCC), and malignant melanoma (MM). However, MM is the main cause of death in patients with skin cancer [3–5]. Early and economical detection of MM is a major public health goal [6]. The increase in exposure to ultraviolet radiation during recent decades has caused a dramatic increase in the incidence of MM. Early diagnosis and surgical removal of cancer resulted in the ten-year survival rate of 70%, in contrast to 20% for those who did not get a diagnosis until the disease was widespread [4].

Currently the method of detecting MM most accepted by dermatologists is dermoscopy used as a diagnostic aid [7–13]. There are two main methods of dermoscopy: using non-polarized light, which requires liquid contact and using polarized light, which is suitable for deeper lesions. Dermatologists diagnose MM according to ABCDE rule (asymmetry, border, color, diameter, and evolution). The major disadvantage of these two types of methods is the heavily dependence on the expertise and training of the dermatologist [14, 15]. Due to this fact, this method causes high rate of false positive alarms. The most common biopsy is excisional biopsy, which is a surgery to remove the whole area of suspicious tissue. Today, in order to avoid unnecessary biopsies (which is an invasive procedure and leaves a scar) [16–21], there are many optical methods that investigate the suspect lesion using higher resolutions. These optical methods, i.e. 'optical biopsy' methods [22,23], such as fluorescence endoscopy [24], optical coherence tomography (OCT) [25,26] and confocal microendoscopy [27,28], were developed in order to extract a three-dimensional cross section, avoiding the diffuse reflected light. However, these methods are very complicated and heavily depend on the expertise of the researcher.

The visual changes (ABCDE) are caused by morphological changes in tumor cells that include alterations of nuclear structure and other cytoplasmic organelles [29–32]. By measuring physical properties of cells and tissue, we have the ability to extract the primary information about these changes before they can even be seen. There are other methods such as the one of Ref [33] which relies on physical measurements, however, these methods are expensive and complicated and therefore are less applicable.

Recently, simple methods for developing a clear image of the nevus using spectro and polarimetric techniques were presented [34–36]. However, the method presented in this paper suggests a new and unique technique in which the physical depth of the nevus tissue is

#253568 Received 9 Nov 2015; revised 14 Jan 2016; accepted 4 Feb 2016; published 24 Feb 2016

directly analyzed by the vibrational responsivity of the tissue. These vibrations characterize the physical properties of the tissue.

The method proposed in this paper relies on the diagnosed of the embroidery vibrations which will be different as a function of the skin growing nature. By extracting this physical character of the embroidery, this method is independence of human visual expertise. We hope that in the next stage our new, very simple and convenient measurement principle for high-precision non-contact remote diagnostics will also be applicable for diagnosis of MM cancer. This development will raise the efficiency of skin self-examination (SSE) using the proposed device.

Our photonic device involves a fast camera and a laser, which is attached to a computing unit. The device is based on tracking the secondary speckle patterns trajectories produced by reflection of an illuminating laser beam from the tissue. This tracking is a technological platform which allows monitoring of movements with nano-metric accuracy.

The tissue is illuminated with a skin safe laser and the reflected secondary speckle patterns are analyzed with a camera [37, 38]. The use of such a concept was already demonstrated for non-contact biomedical monitoring including different biomedical parameters such as heart rate [39], non-invasive monitoring of glucose concentration in blood [40,41], remote estimation of alcohol in blood stream [42], blood pulse pressure [43] and measurement of intra ocular pressure [43,45].

In this paper we present the theoretical concept and perform experimental validation of the speckle based sensing technology for non-contact detection of pigmentary lesion. This article describes the ability to characterize pigmented lesions, which is a preliminary stage for the characterization of melanoma.

2. Theoretical explanation

The temporal movements of pigmentary lesions are produced due to acoustic vibrations of a controlled vibration surface (CVS) that we generate by loud speaker positioned in proximity to the inspected skin. The CVS induces skin and pigmentary lesions vibrations as a function of the skin density. The described configuration includes observation of the secondary speckle pattern that is created by illuminating the nevus. In order to monitor the nevus vibration, the correlation of each of the sequential images is measured. By analyzing the change in the correlation peak position, relative movement of the stimulated nevus was extracted as is shown in Fig. 1. The amplitude of the vibrations was measured with the presented technology which is considered to be very precise (nanometric resolution). The sensitivity of the presented approach was proven several times before with different conditions as it is shown in Refs [37–45]. Summary of the process is shown in Fig. 2.

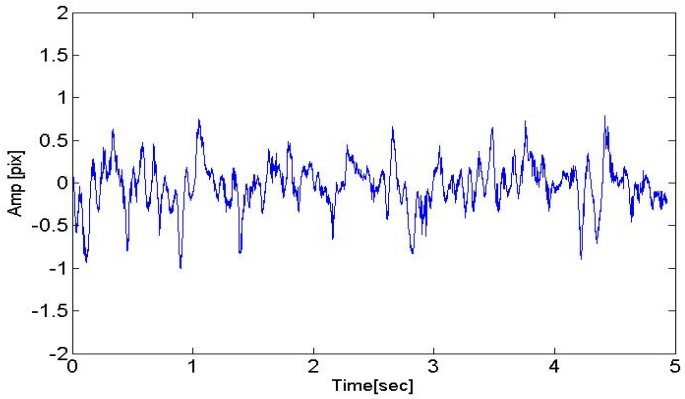

Fig. 1. The temporal change in the position of the correlation peak (in pixels) versus time.

#253568 Received 9 Nov 2015; revised 14 Jan 2016; accepted 4 Feb 2016; published 24 Feb 2016

The relative shift of the speckle pattern is proportional to [11]:

$$\beta = \frac{4\pi \tan\alpha}{\lambda} \approx \frac{4\pi\alpha}{\lambda} \tag{1}$$

where α is the time varying tilting angle of the illuminated surface as is shown in Fig. 3, β is proportional to the change in the spatial position of the speckle pattern due to the pigmentary lesion's temporal movement, λ is the illumination wavelength, which in our case was 532 nm. The chosen wavelength of the illumination is related to the fact that the presented paper examined the difference between normal skin tissues and pigmented lesion. The penetration depth of 532nm wavelength is enough in order to detect pigmented lesion (which not penetrate the whole epidermis). The wavelength of 630nm was also suitable due to the same reason. The temporal movement of the pigmentary lesion is proportional to the change in the speckle pattern that is caused by the CVS vibrations.

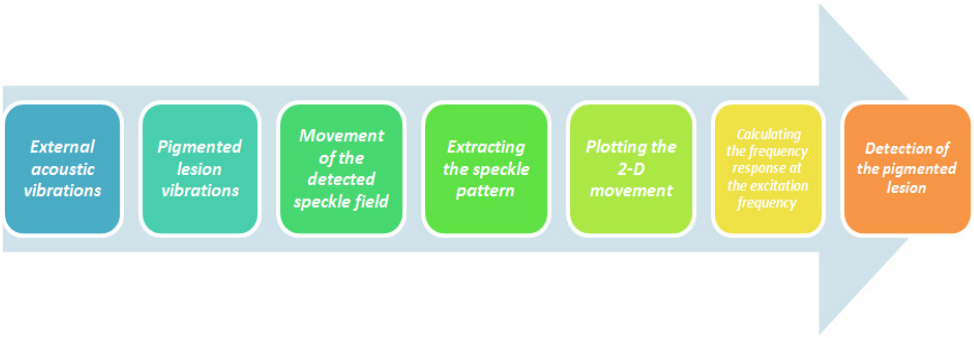

Fig. 2. A flowchart of the pigmentary lesion effects on the speckle pattern vibrations.

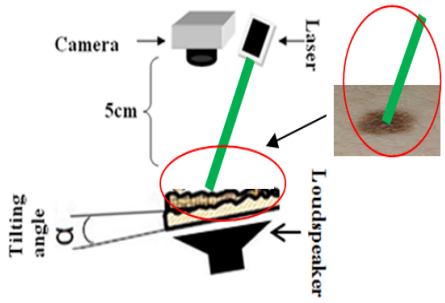

Fig. 3. Schematic diagram of the system.

In order to detect a pigmentary lesion we calculated the frequency response of the pigmentary lesion at the excitation vibration frequencies (main peak) when vibrated due to the CVS excitation. The frequency response is expressed as a discrete Fourier transform (DFT):

$$X(k) = \sum_{j=1}^{N} x(j) \cdot e^{-2\pi ijk/N} \tag{2}$$

where x(j) is a temporal vector of the changes in the position of the correlation peak versus time, N is the number of frames that were captured during each sample and X(k) is the frequency response raw data. An example of the pigmentary lesion frequency response with respect to a skin area without any pigmentary lesion is shown in Fig. 4. The result is similar to

#253568 Received 9 Nov 2015; revised 14 Jan 2016; accepted 4 Feb 2016; published 24 Feb 2016

a Bode diagram where the amplitude of different vibration modes is measured in pixel's shift of the correlation peak. One can see that pigmentary lesion provides a vibration spectrum with peak at 170 Hz (the excitation frequency) with a different amplitude from the control one (i.e. the regular skin tissue) at the same extrication frequency (170 Hz).

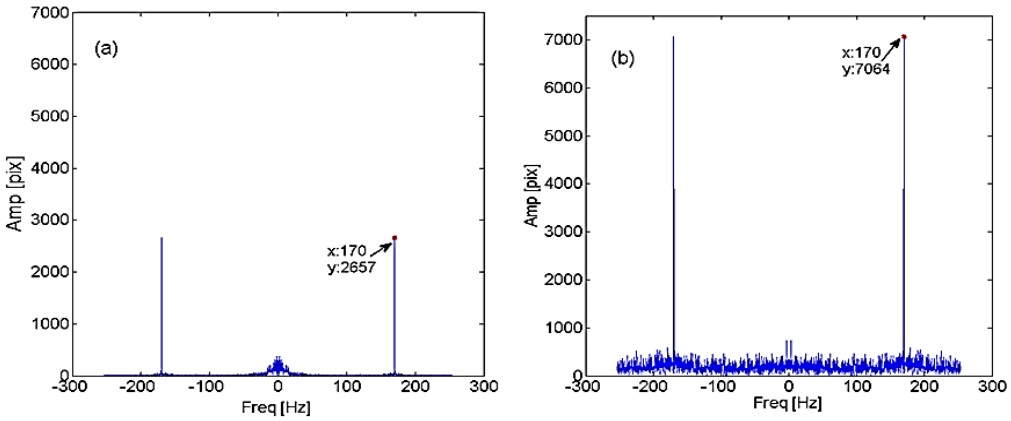

Fig. 4. (a) Frequency response of a pigmentary lesion. (b) Frequency response of skin area without any pigmentary lesion. The excitation frequency during this experiment is 170 Hz.

3. Experimental results

The setup is a device that includes the following components: (1) a camera (PixelLink PL-E531) that captures images of the secondary speckle pattern reflected from the subject's hand at the rate of 500 frames per second (fps), the camera is connected to a computer. The distance from the camera to the subject's hand is approximately 5cm. (2) a green laser (at wavelength of 532nm) with output power of 2mW. Note that the speckle patterns trajectory was also clearly observed with a low power laser (<0.5mW). In all cases we do not recommend directing the laser towards eyes and we recommend use of appropriate eye protection. The vibrations were generated through a Matlab code program, while the output source was connected through the USB cable. In order to obtain vibrations a loud speaker that the subject wears like a bracelet (Fig. 5(a)) was used. The change in the 2-D position of the correlation peak versus time due to the CVS vibrations was calculated after extracting the speckle pattern in each frame as it is shown in Fig. 5. In most of the measurements, the laser beam was smaller than the pigmented lesion size. However, please note that the important physical parameter of MM and pigmented lesions is the depth of the pigmented area. As it will be shown, the results demonstrate that even while the illuminated beam was bigger than the pigmented area, the vibrations characteristics were significantly changed due to the difference between the depth of the pigmented lesion and a normal skin tissue.

#253568 Received 9 Nov 2015; revised 14 Jan 2016; accepted 4 Feb 2016; published 24 Feb 2016

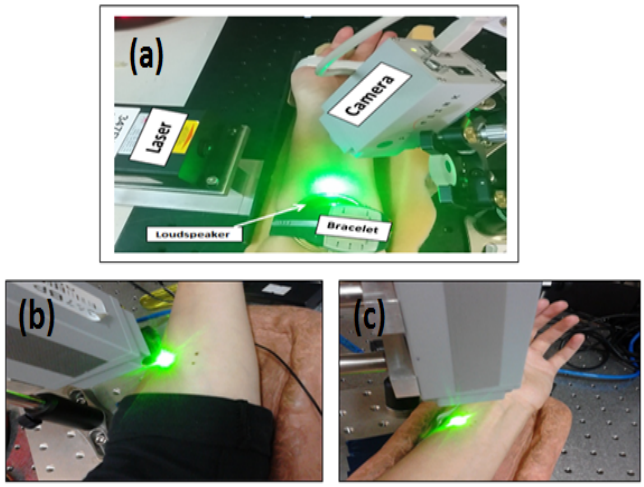

Fig. 5. (a) The optical configuration for remote measuring of pigmentary lesion. (b) Reference spot of normal skin is positioned under a laser illumination. (c) Demonstration of a pigmentary lesion under illumination.

3.1. Stability test

The stability of normal skin (i.e. without any pigmentary lesion) was checked to quantify the performance of the device and to ensure that the changes on the frequency response were indeed the result of a pigmentary lesion with respect to normal skin. During the stability test a spot of normal skin was examined while the CVS of the subject's hand was at 170 Hz. After each measurement the subject's hand was removed and returned approximately to the same location. This procedure was repeated eleven different times. The results were normalized to the first frequency response. One can see in Fig. 6 that the STD (standard deviation) of the normalized frequency response is only 11.1%. The STD of the samples, was calculated by:

$$s = \left(\frac{1}{N-1} \sum_{n=1}^{N} (x_n - \bar{x})^2 \right)^{0.5} \tag{3}$$

where $\bar{x} = 1/N \sum_{n=1}^{N} x_n$ and N is the number of elements in the sample

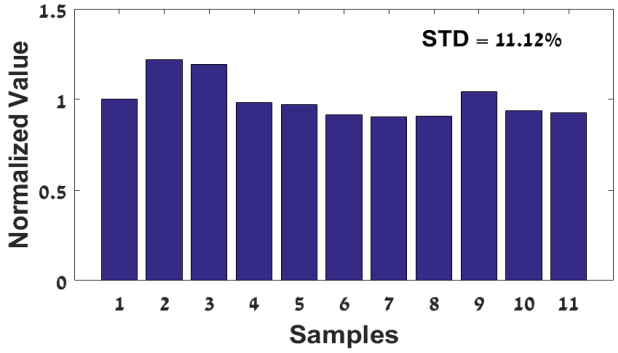

Fig. 6. Stability test of the system: The normalized optical parameter versus 10 different samples taken while a normal spot of the skin is under illumination. The STD is displayed.

#253568 Received 9 Nov 2015; revised 14 Jan 2016; accepted 4 Feb 2016; published 24 Feb 2016

3.2 Signature of pigmentary lesion and normal skin

The main test was divided into 2 parts. Initially, experiments were done on the same subject, while we examined one single pigmented lesion spot with respect to nine different normal skin spots. The first step was to apply different frequencies using the CVS. After extracting the speckle pattern in each frame, we calculate the correlation and obtain a change in the 2-D position of the correlation peak versus time. One can see in Fig. 7 the raw data of 2-D correlation images sequence of the five different frequencies.

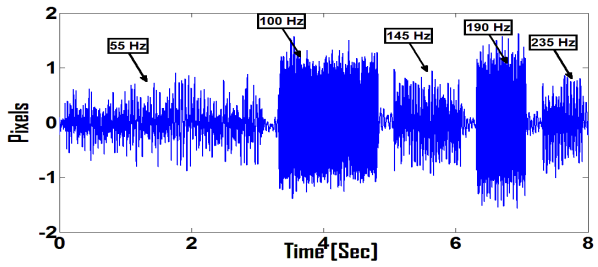

Fig. 7. The time domain response to the series of different vibration frequencies applied by the CVS.

The next step was to analyze each sequence of different frequency separately. One can see in Fig. 8 the different vibrations of the skin for each and different applied frequency.

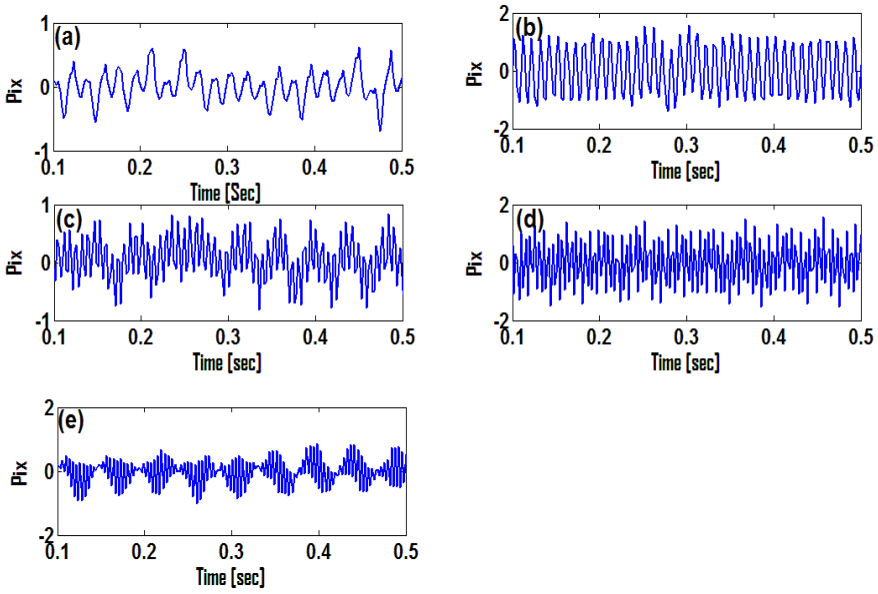

Fig. 8. Different temporal vibrations of the skin while frequency of (a) 55 Hz (b) 100 Hz (c) 145 Hz (d) 190 Hz (e) 235 Hz was applied by the CVS.

After each time-domain sequence was extracted, we calculated the frequency response of each different sequence as it is shown in Fig. 9. One can see from the symmetry of the frequency response that the signal is real and the excited frequency response can be easily extracted with very high signal to noise ratio (SNR).

#253568 Received 9 Nov 2015; revised 14 Jan 2016; accepted 4 Feb 2016; published 24 Feb 2016

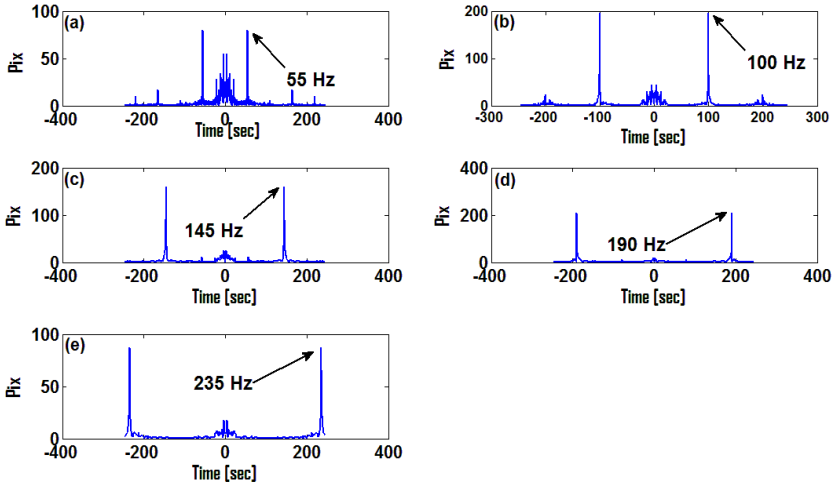

Fig. 9. Different frequency responses of the skin while frequency of (a) 55 Hz (b) 100 Hz (c) 145 Hz (d) 190 Hz (e) 235 Hz was applied by the CVS.

Finally, by calculating the peak of each frequency response at the tremor frequency, a unique signature was created as it shown in Fig. 10. With the signature, one can classify the skin condition, due to the fact that the skin vibration behavior changes as a function of the pigmented lesion characteristics and can be analyzed using the frequency response signature.

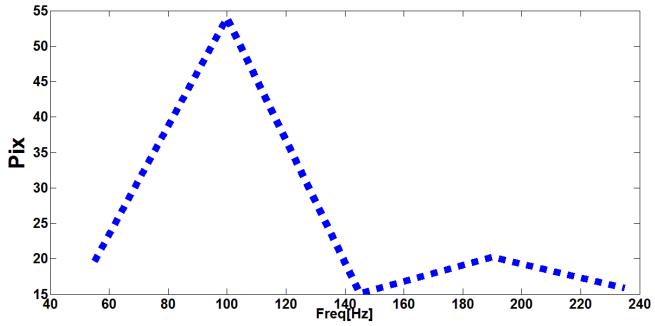

Fig. 10. The frequency response signature of a normal skin.

During the first step one can see (Fig. 11) the different signature of nine different normal skin spots with respect to a single pigmentary lesion spot.

#253568 Received 9 Nov 2015; revised 14 Jan 2016; accepted 4 Feb 2016; published 24 Feb 2016

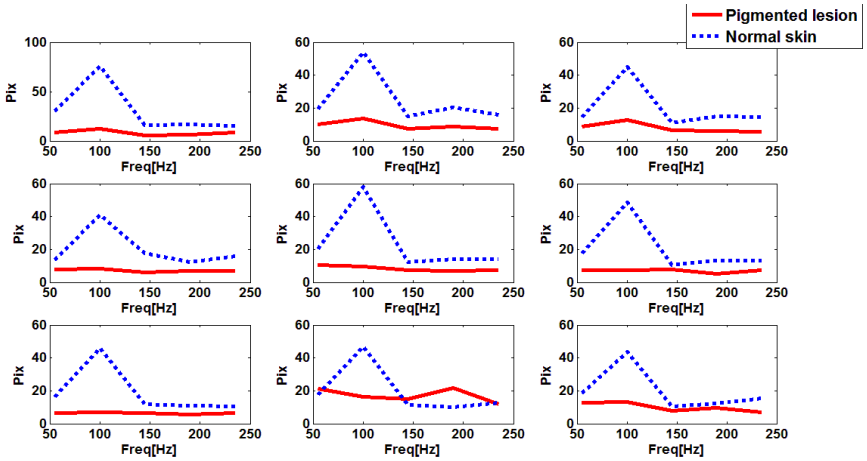

Fig. 11. Nine different optical signatures of different skin spots with respect to a pigmented lesion spot. The optical measurement of the pigmented lesion is denoted with a red line and the optical measurement of the normal skin is denoted with a blue dashed line.

One can see that at an excited frequency of 100Hz there is a significant difference between each one of the nine normal skin spot to the pigmented lesion spot. The presented resonance frequencies are related to two main factors: (1) The loudspeaker's resonance and (2) the mechanical properties of the vibrated tissue, which affect the interaction between the acoustic wave and the tissue. One can see from Fig. 13 that the resonance of the loudspeaker is at about 100Hz. However, the difference between soft tissue and hard tissue as it is expressed by the difference between pigmented lesions to normal skin, affects the resonance. This phenomenon (i.e. the frequency response difference between hard and soft tissues) was also proved in Ref [37]. Please note that the range of the excited frequencies is also limited by the frame rate of the camera due to the Nyquist sampling theorem.

Figure 11 represents one single pigmented lesion. However, each time, the subject moved his arm and placed his arm back again for repetition, the movement caused to slight changes of the signature. One can see that the signature remains the same with respect to the other skin frequency responses. In the last step, we calculate the STD of the pigmented lesion signature result at the excitation frequencies and we saw that the optical measurements of the normal skin were out of the pigmented lesion deviation region as it is shown in Fig. 12.

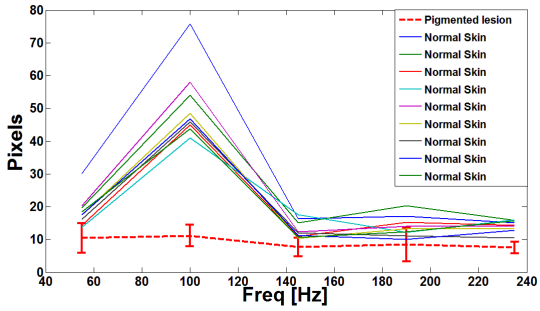

Fig. 12. The signature deviation of the pigmented lesion optical measurement with respect to nine different optical measurements of normal skin. The optical measurement of the pigmented lesion is denoted with a red dashed line.

During the second test, we tested whether pigmentary lesion can be characterized in relation to their environment by using our system. For our tests, the excitation frequency was at 55-240Hz. Different pigmentary lesions, with different appearance, were examined. Each

#253568 Received 9 Nov 2015; revised 14 Jan 2016; accepted 4 Feb 2016; published 24 Feb 2016

test presents the measurements obtained from observing three samples of single normal skin with respect to three measurements of single pigmentary lesion. In Fig. 13 we present 6 different pairs of pigmentary lesion signatures and normal skin signatures. The pigmented lesions of the subjects were analyzed by a dermatologist and were not detected as MM.

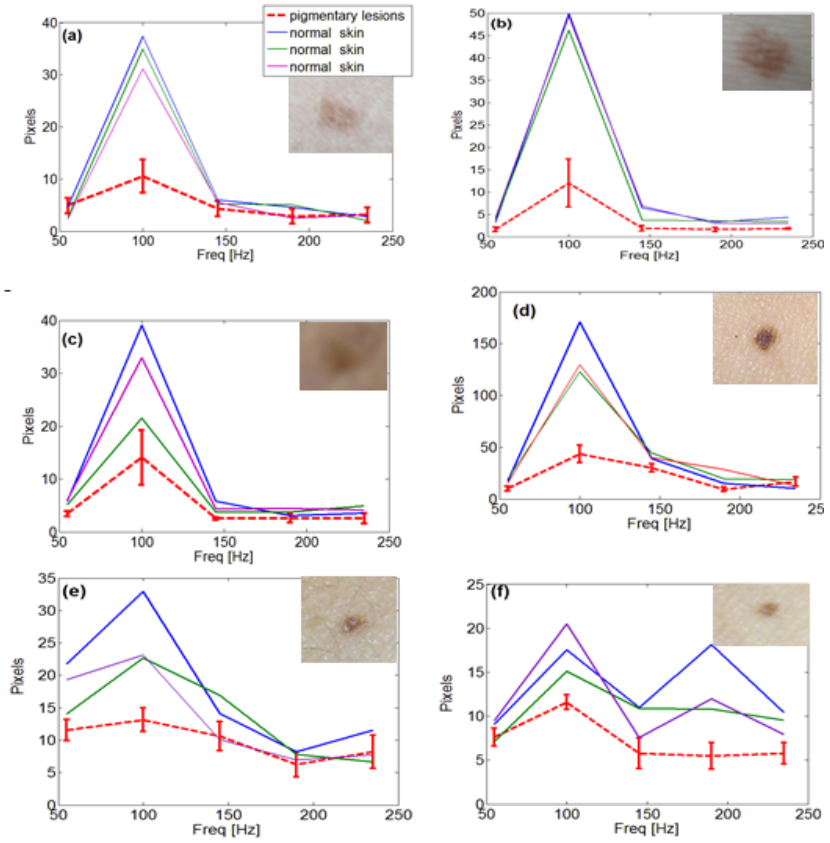

Fig. 13. Six different signatures of skin tissues.

3.3 Examination of skin spots, pigmented spots and colored spots

In the second part of the study the frequency response of 20 different small and flat pigmented lesions was examined. The excitation frequency was between 170Hz to 210Hz. The excitation frequency was selected due to the observation of small and flat pigmented lesions frequency response. The difference at this excitation frequency can be seen in Fig. 14.

The parameters that were examined were chosen in order to evaluate our ability to monitor pigmentary lesion with the proposed optical system. 'Color' - The skin area is illuminated as a reference was painted with a color matching to the Nevus color. This was done to ascertain that the different frequency responses between real pigmentary lesion and the reference are not only due to different color of the skin. 'Control' – the spot of a normal skin with neither pigmentary lesion nor color was illuminated. Each pigmented lesion and colored spot measurement was normalized by the measurement of the adjacent normal skin and the ratio was presented in the manuscript.

The difference in frequency response between colored, non-colored and the pigmentary lesion is evident from the graph of Fig. 14. In all cases calibration was done in relation to their control. The results show that by selecting the suitable threshold, one can easily diagnose a pigmentary lesion or mole with the presented method (e.g. a difference of 400

#253568 Received 9 Nov 2015; revised 14 Jan 2016; accepted 4 Feb 2016; published 24 Feb 2016

pixels at 170Hz, as shown in Fig. 4). As one can see from Fig. 14, that there is a small difference between the colored spot frequency responses and a normal skin with respect to the ratio between pigmented lesions to colored spot. In order to avoid movements and external noises, the comparison was made between adjacent normal skin spot, while one of them is colored. Due to this fact, there is a small difference in the frequency response between the colored spots and the non-colored ones.

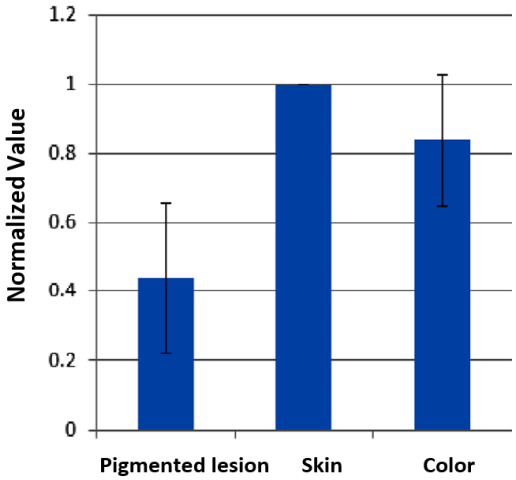

Fig. 14. The average frequency responses of 20 different small pigmented lesions with respect to reference spots after calibration. The responses are measured at frequencies of 170Hz and 210Hz.

4. Conclusions

In this paper we presented the usage of optical remote configuration that relies on the physical response of the tissue for detection of pigmentary lesions. The proposed configuration consists of only a camera, a laser and a small loud speaker. The proposed novel concept was experimentally validated and demonstrated its potential in detection of pigmentary lesions.

The next step will be developing an automatic calibration process that will improve the translation of the optical result into the exact diagnosis of malignant melanoma.

The future sensor will be very simple, extremely compact, suitable for personal use, robust and will be automatic and independent of physician's visual examination. Due to this fact the false alarm rate will be significantly reduced with respect to nowadays false alarm rate. Furthermore, the laser is considered very safe due to the fact that its output optical power can be less than 0.4mW.

#253568 Received 9 Nov 2015; revised 14 Jan 2016; accepted 4 Feb 2016; published 24 Feb 2016